DOI:10.1021/jf103116c

JOURNAL OF AGRICULTURAL AND FOOD CHEMISTRY
ARTICLE

Formation of Arginine Modifications in a Model System of N^{α}-*tert*-Butoxycarbonyl (Boc)-Arginine with Methylglyoxal

Antje Klöpfer, Robert Spanneberg, and Marcus A. Glomb*

Institute of Chemistry, Food Chemistry, Martin-Luther-University Halle-Wittenberg, Kurt-Mothes-Strasse 2, 06120 Halle/Saale, Germany

The present study deals with the mechanistic reaction pathway of the α-dicarbonyl compound methylglyoxal with the guanidino group of arginine. Eight products were formed from the reaction of methylglyoxal with N^{α}-*tert*-butoxycarbonyl (Boc)-arginine under physiological conditions (pH 7.4 and 37 °C). Isolation and purification of substances were achieved using cation-exchange chromatography and preparative high-performance liquid chromatography (HPLC). Structures were verified by nuclear magnetic resonance (NMR) and high-resolution mass spectrometry. 2-Amino-5-(2-amino-4-hydro-4-methyl-5-imidazolinone-1-yl)pentanoic acid (**3**) was determined as the key intermediate precursor within the total reaction scheme. Kinetic studies identified N^{δ}-(5-methyl-4-oxo-5-hydroimidazolinone-2-yl)-L-ornithine and N^{7}-carboxyethylarginine as thermodynamically more stable products from compound **3**. Further mechanistic investigations revealed an acidic hydrogen at C-8 of compound **3** to trigger aldol condensations. This reactivity of compound **3** allowed for the addition of another molecule of methylglyoxal to form products, such as N^{δ}-(4-carboxy-4,6-dimethyl-5,6-dihydroxy-1,4,5,6-tetrahydropyrimidine-2-yl)-L-ornithine and argpyrimidine.

KEYWORDS: Methylglyoxal−arginine modifications; Maillard reaction; N^{7}-(1-carboxyethyl)arginine; 2-amino-5-(2-amino-4-hydro-4-methyl-5-imidazolinone-1-yl)pentanoic acid

INTRODUCTION

Reactive α-dicarbonyl compounds, such as methylglyoxal (MGO), formed in early stages of the Maillard reaction are potent protein modifiers. Quantification of MGO was performed in foods and also in *in vivo* samples. In coffee, wine, and apple juice, levels up to 25 ppm were analyzed (*1*). Very high amounts of MGO (761 ppm) were measured in honey samples from New Zealand (*2*). Blood levels of diabetic patients demonstrate the physiological relevance of MGO. In contrast to normal controls (256 ± 92 nM), concentrations of 479 ± 49 nM were found (*3*).

Five mechanisms of formation have been elucidated for MGO. An important source is the Maillard reaction of reducing sugars with amines. At early stages, dicarbonyl is formed during degradation of fructosamine or the reverse aldol reaction of 3-deoxyglucosone (*4*). *In vivo*, both the enzymatic and non-enzymatic elimination of phosphate from glycerine-3-phosphate or dihydroxyacetonphosphate is a main step for the generation of MGO (*5*, *6*). Furthermore, cytochrome P450 2E1 catalyzes the formation from acetone and represents an additional physiological source (*7*). Another formation pathway is described from the oxidation of aminoacetone during the catabolism of threonine (*8*).

As a highly reactive α-dicarbonyl compound, MGO reacts with the ε-amino group of lysine to form N^{ε}-(carboxyethyl)lysine (CEL) (*9*) and the imidazolium cross-link 2-ammonio-6-[1-(5-ammonio-6-oxido-6-oxohexyl)-5-methylimidazolium-3-yl]-hexanoate (MOLD) (*10*). The reaction of MGO with both arginine and lysine leads to a cross-link structure that has been described as 2-ammonio-6-({2-[(4-ammonio-5-oxido-5-oxopentyl)-amino]-4-methyl-4,5-dihydro-1*H*-imidazol-5-ylidene}-amino)-hexanoate (MODIC) (*11*). From the reaction of MGO with the guanidino group of arginine, six products have been established in the literature. Henle et al. identified protein-bound imidazolinone N^{δ}-(5-methyl-4-oxo-5-hydroimidazolinone-2-yl)-L-ornithine with N^{δ} exocyclic (MG-H1) (**2**) (*12*). Two other imidazolinone structures, 2-amino-5-(2-amino-5-hydro-5-methyl-4-imidazolon-1-yl)pentanoic acid (MG-H2) and 2-amino-5-(2-amino-4-hydro-4-methyl-5-imidazolon-1-yl)pentanoic acid (MG-H3) (**3**) with N^{δ} endocyclic, were synthesized and characterized by Ahmed et al. (*13*). The open-chain compound N^{7}-(1-carboxyethyl)arginine (**6**) was synthesized under high hydrostatic pressure by Alt and Schieberle (*13*). Products generated from two molecules, MGO and arginine, are N^{δ}-(4-carboxy-4,6-dimethyl-5,6-dihydroxy-1,4,5,6-tetrahydropyrimidine-2-yl)-L-ornithine (**1**) (*14*) and argpyrimidine (**5**) (*15*).

In the literature, little is known about the detailed formation pathways of MGO−arginine modifications and their exact mechanistic relationship. Therefore, we started to reinvestigate this aspect of the Maillard reaction, including isolation and characterization of the key players, and separate incubations of isolated structures. With respect to the many structures and countless different incubation setups published in the literature and to compare results with previous investigations of our working group on glyoxal−arginine reactions, a simple model system of equimolar concentrations of N^{α}-*tert*-butoxycarbonyl (Boc)-arginine and MGO was used.

MATERIALS AND METHODS

Materials. Chemicals of the highest quality available were obtained from Aldrich (Taufkirchen, Germany), Fluka (Taufkirchen, Germany),

*To whom correspondence should be addressed. Fax: ++49-345-5527341. E-mail: marcus.glomb@chemie.uni-halle.de.

 Published on Web 12/02/2010

Merck (Darmstadt, Germany), Roth (Karlsruhe), and Sigma (Taufkirchen, Germany), unless otherwise indicated.

Synthesis. Substances **1**, **2**, **3**, **4**, **6**, **7**, and **8** were isolated from incubations of 220 μL (1.4 mmol) MGO (40% commercial solution) and 213 mg (1.2 mmol) L-arginine in 10 mL phosphate buffer (0.2 M, pH 7.4). Reaction mixtures were incubated for 4.5 h at 40 °C. Subsequently, the pH was adjusted to 4.0 with 1 N HCl. A total of 8 mL of the solution was adjusted to pH 1 with 1 N HCl and subjected to ion-exchange chromatography. Fractions were collected and analyzed by thin-layer chromatography (TLC) and analytical high-performance liquid chromatography (HPLC). After removal of solvents, residues were dissolved in H_2O and subjected to preparative HPLC. Desired substances were collected and freeze-dried (freeze-drying device, VirTis Benchtop SLC, Warminster, PA). Substance **5** (argpyrimidine) was synthesized according to Shipanova et al. (*15*).

MGO. To eliminate side reactions between products of MGO and arginine with contaminants in the commercial MGO solution, it was necessary to synthesize highly purified MGO. The synthesis was based on a method by McLellan and Thornalley (*16*). A total of 5 mL (41.31 mmol) of pyruvic aldehyde dimethyl acetal (97%) was dissolved in 100 mL of aqueous sulfuric acid (5%, v/v) and heated over 1 h in a boiling water bath. Subsequently, the mixture was distilled fractionally on a 34 × 1.5 cm inner diameter column under reduced pressure (30 mbar) and nitrogen bleed. Three fractions (boiling point of the azeotrope = 26 °C) were collected and filled up to 100 mL. The concentrations were determined by derivatization with 1,2-phenylenediamine and HPLC analysis.

N^{δ}-(4-Carboxy-4,6-dimethyl-5,6-dihydroxy-1,4,5,6-tetrahydropyrimidine-2-yl)-L-ornithine (***1***). After ion-exchange chromatography, fractions with material having R_f = 0.33 were verified by analytical HPLC (t_R = 18.6 min, isocratic elution with 2% solvent B) and the procedure was continued as described above. Preparative HPLC and subsequent freeze-drying gave a colorless amorphic material (71.55 mg, 14.2%, **1** + 2HFBA salt based on elemental analysis). The chemical structure was confirmed by ^{1}H and ^{13}C nuclear magnetic resonance (NMR), and results were similar to those from Oya et al. (*14*).

Accurate mass (mean of three measurements ± standard deviation) *m*/*z*: $[M + H]^+$ 319.1614 ± 0.0006 (319.1612, calcd for $C_{12}H_{23}N_4O_6$).

N^{δ}-(5-Methyl-4-oxo-5-hydroimidazolon-2-yl)-L-ornithine (***2***). After ion-exchange chromatography, fractions with material having R_f = 0.48 were verified by analytical HPLC (t_R = 72.7 min, isocratic elution with 2% solvent B) and the procedure was continued as described above. Preparative HPLC and subsequent freeze-drying gave a colorless amorphic material (49.22 mg, 11.6%, **2** + 2HFBA salt based on elemental analysis). The chemical structure was confirmed by ^{1}H and ^{13}C NMR and high-resolution mass spectrometry. The results were similar to those from Henle et al. (*12*).

Accurate mass (mean of three measurements ± standard deviation) *m*/*z*: $[M + H]^+$ 229.1314 ± 0.0007 (229.1312, calcd for $C_9H_{17}N_4O_3$).

2-Amino-5-(2-amino-4-hydro-4-methyl-5-imidazolinone-1-yl)pentanoic Acid (***3***). After ion-exchange chromatography, fractions with material having R_f = 0.47 were verified by analytical HPLC (t_R = 74.4 and 78.2 min, isocratic elution with 2% solvent B) and the procedure was continued as described above. A colorless amorphic material (25.67 mg, 11.1%, **3** + 2HFBA salt based on elemental analysis) was obtained by preparative HPLC and subsequent freeze-drying. The chemical structure was confirmed by ^{1}H and ^{13}C NMR and high-resolution mass spectrometry. NMR data gave similar results to those from Ahmed et al. (*13*).

Accurate mass (mean of three measurements ± standard deviation) *m*/*z*: $[M + H]^+$ 229.1301 ± 0.0008 (229.1299, calcd for $C_9H_{17}N_4O_3$).

2-Amino-5-(2-amino-4-methyl-4-(methyl-ol)-5-imidazolinone-1-yl)-pentanoic Acid (***4***). After ion-exchange chromatography, fractions with material having R_f = 0.50 were verified by analytical HPLC (t_R = 89.9 min, isocratic elution with 2% solvent B) and the procedure was continued as described above. Preparative HPLC and subsequent freeze-drying gave a colorless amorphic material (60.00 mg, 12.5%, **4** + 2HFBA salt based on elemental analysis). The chemical structure was confirmed by ^{1}H and ^{13}C NMR and high-resolution mass spectrometry.

^{1}H NMR (400 MHz, CD_3OD) δ (ppm): 3.85 (t, ^3J = 5.89 Hz, 1H, H-2), 1.7−1.9 (m, 2H, H-3), 1.5−1.7 (m, 2H, H-4), 3.56 (t, ^3J = 6.53 Hz, 2H, H-5), 1.19 (s, 3H, H-9), 3.67, (t, ^3J = 7.12 Hz, 2H, H-10). ^{13}C NMR (400 MHz, CD_3OD) δ: 171.23 (C-1), 52.20 (C-2), 26.63 (C-3), 22.81 (C-4), 38.97 (C-5), 157.43 (C-6), 176.46 (C-7), 66.01 (C-8), 16.91 (C-9), 64.48 (C-10).

Accurate mass (mean of eight measurements ± standard deviation) *m*/*z*: $[M + H]^+$ 259.1412 ± 0.0010 (259.1414, calcd for $C_{10}H_{19}N_4O_4$).

Model Reactions. In general, experiments were conducted in 0.2 M phosphate buffer.

N^{α}-t-Boc-Arginine−MGO Incubations. For mechanistic investigations, incubations of 20 mM MGO (commercial and synthetic) with 20 mM N^{α}-*t*-Boc-arginine were performed at pH 5.0, 7.4, and 8.5 at 37 °C. To stop the reaction and for removal of the protection group, aliquots of a well-defined volume were taken at several times and the same volume of 6 N HCl was added. After 30 min, the samples were diluted for HPLC analysis.

Incubation of Isolated Structures. Further information about the mechanisms was revealed by incubation of the separated compounds at pH 5.0, 7.4, and 8.5 at 37 °C. Structures were dissolved in phosphate buffer. To stop the reaction, samples were diluted with 0.05 M HCl and analyzed by HPLC and post-column derivatization.

Incubations of Isolated Structures with Carbonyl and Dicarbonyl Compounds. Mechanistic insights were obtained from incubation of compounds **2** and **3** with formaldehyde or MGO. Both structures (5 mM) were incubated at pH 5.0, 7.4, and 8.5 at 37 °C with 2.5 mM formaldehyde or MGO. The reaction was stopped by diluting the samples for HPLC analysis with 0.05 M HCl.

Statistics. Data shown for model reactions resulted from at least three independent incubations and gave coefficients of variations < 5%.

Chromatography. TLC was performed on silica gel 60 F_{254} plates (Merck) with 4:2:3:3 *n*-butanol/H_2O/HOAc/pyridine as the mobile phase. Visualization of separated material was achieved with ninhydrin.

Ion-exchange chromatography was performed on Dowex 50WX4-400 (2.5 cm inner diameter × 22 cm, H^+ form). Before conditioning with pyridinium formiate (0.2 M, pH 5.0), the column was washed with 1 M NaOH, 1 M HCl, and water.

Solvents were all chromatographic-grade. From the individual chromatographic fractions, solvents were removed under reduced pressure.

HPLC. *Analytical System*. A Jasco (Gross-Umstadt, Germany) ternary gradient unit 980-PU-ND with degasser DG-980-50, autosampler 851-AS, column oven set at 20 °C, and fluorescence detector FP-920 was used. Chromatographic separations were performed on stainless-steel columns (YMC Hydrosphere C18, 250 × 4.6 mm, Dinslaken, Germany) using a flow rate of 1.0 mL/min. The mobile phase used was water (solvent A) and MeOH/water (7:3, v/v; solvent B). To both solvents (A and B), 1.2 mL/L heptafluorobutyric acid (HFBA) was added. Samples were injected at 2% B and run isocratic for 80 min, and then the gradient changed to 100% B in 5 min and held at 100% for 20 min. For better separation, the ratio of solvent B was decreased to 2%. Samples were analyzed isocratic as well. The fluorescence detector was attuned to 340 nm for excitation and 455 nm for emission. Prior, a post-column derivatization reagent was added at 0.5 mL/min. This reagent consisted of 0.8 g of *o*-phthaldialdehyde, 24.73 g of boric acid, 2 mL of 2-mercaptoethanol, and 1 g of Brij35 in 1 L of H_2O adjusted to pH 9.75 with KOH.

For determination of argpyrimidine (**5**), samples were measured without post-column derivatization after separation by a gradient chromatography program (7% B changed in 60 min to 90% B). The fluorescence detector was set to 320 nm for excitation and 380 nm for emission.

Preparative System. A Besta HD 2-200 pump (Wilhelmsfeld, Germany) with a Gynkotek fluorescence detector RF-530 and a SERVOGOR 220 pen recorder was used. Chromatographic separations were performed on a stainless-steel column (VYDAC 218TP1022, 250 × 25 mm, RP18, 10 μm) using a flow rate of 15 mL/min. The mobile phase was identical to the analytical HPLC system, using a composition of 5% solvent B and isocratic gradient. The effluent was split and adjusted to a post-column derivatization, as described under the analytical HPLC system. Fractions with material were collected, combined, and freeze-dried as described under Synthesis.

HPLC−Electrospray Ionization−Mass Spectrometry (HPLC−ESI−MS). As described above, the same analytical HPLC system was used to separate the different structures. The mass spectra were obtained from an Applied Biosystems 4000 Q Trap linear ion trap quadrupole LC/MS/MS with a Turbo Spray source at positive-ion mode. The source

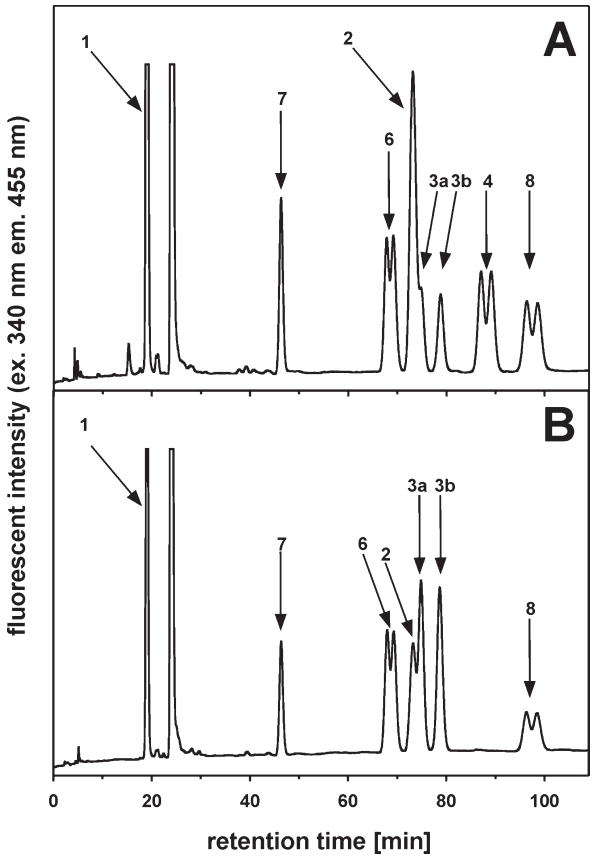

Figure 1. HPLC chromatogram obtained with fluorescence detection after post-column derivatization with *o*-phthaldialdehyde of incubation of N^{α}-*t*-Boc-arginine (20 mM) with MGO (20 mM) after 24 h at 37 °C and pH 7.4: (**A**) incubation with commercial MGO and (**B**) incubation with synthesized MGO.

was maintained at a voltage of 3.5 kV and a nebulizer gas flow of 60 μL/min with a declustering potential of 50 V. For MS/MS experiments, the entrance potential of the collision cell was 9 V, the exit potential was 30 V, and the collision energy was 33 V.

Accurate Mass Determination. For accurate mass determination, a Micromass (Manchester, U.K.) VG platform II quadrupole mass spectrometer equipped with an ESI interface was employed: ESI^+; source temperature, 80 °C; capillary, 3.0 kV; and cone voltage, 20 V. The data were collected in the multichannel acquisition (MCA) mode with 128 channels per *m*/*z* unit using 13 scans (6 s) with 0.1 s reset time. The resolution was 650 (10% valley definition). The sample was dissolved for analysis in water/MeCN (1:1) containing poly(ethylene glycol) (PEG) 200 (0.1 μg/μL) as the reference material, ammonium formate (0.1%), and formic acid (0.2%). The sample concentration was similar to that of PEG 200. The solution was introduced into the ESI source at a flow of 5 μL/μmin. With a *m*/*z* 190−285 scan range, five reference peaks could be used for calibration: *m*/*z* 195.1234, 212.1498, 239.1495, 256.1760, and 283.1757.

NMR Spectroscopy. NMR spectra were recorded on Varian Unity Inova-500 and Varian Gemini 2000 instruments (Darmstadt, Germany). Chemical shifts are given relative to external Me_4Si.

RESULTS

Isolation and Characterization of Products. In the reaction of MGO with N^{α}-*t*-Boc-arginine, eight products were formed after 24 h (**Figure 1A**). Compounds **1**, **2**, **3**, and **4** were isolated by ion-exchange chromatography. Final purification was performed by ion-pair chromatography on reversed-phase material. Structural evidence was achieved by ^1H and ^{13}C NMR, as well as heteronuclear multiple-quantum coherence (HMQC) and heteronuclear multiple-bond correlation (HMBC) NMR experiments. Accurate mass detection confirmed the chemical structures. The data unequivocally identified compound **1** as N^{δ}-(4-carboxy-4,6-dimethyl-5,6-dihydroxy-1,4,5,6-tetrahydropyrimidine-2-yl)-L-ornithine. Compound **2** was determined as N^{δ}-(5-methyl-4-oxo-5-hydroimidazolon-2-yl)-L-ornithine. Compounds **3a** and **3b** are two possible diasteriomeric isomers of 2-amino-5-(2-amino-4-hydro-4-methyl-5-imidazolon-1-yl)pentanoic acid. Isolated compound **4** was characterized as the diastereomeric aldol addition products of compound **3** and formaldehyde. The $^3J_{H\text{-}5,C\text{-}7}$ correlation indicated a N^{δ}-endocyclic ring structure. Moreover, correlation $^3J_{H\text{-}10,C\text{-}7}$ showed the addition of formaldehyde at the C-8 position of compound **3**. The assumption that this product was formed from formaldehyde in commercially available MGO solution was proved by an experiment with independent synthesized MGO, as described by McLellan and Thornalley (*16*). Incubation of purified MGO with N^{α}-*t*-Boc-arginine led to the same product profile as shown in **Figure 1A**, except for compound **4** (**Figure 1B**). This result led to the conclusion that compound **4** is an artifact formed by impurities of formaldehyde in the model reaction system with commercial MGO.

Compound **5** was determined as argpyrimidine by HPLC with fluorescence detection and a comparison to the synthesized standard, as described by Shipanova et al. (*15*). Compound **6** was identified as N^7-carboxyethylarginine by HPLC−ESI−MS analysis with *m*/*z* 247 [M + 1].

HPLC−ESI−MS analysis revealed *m*/*z* 319 for both signals **7** and **8**. Isolation of compounds **7** and **8** by ion-exchange chromatography and purification by preparative HPLC was not successful. HPLC of collected fractions always showed a 1:1 equilibrium of both structures besides other unidentified material. Because derivatization with *o*-phthaldialdehyde was reported to lead to a comparable molar response in fluorometric analysis, quantitative results for compounds **7** and **8** were obtained using a standard solution of compound **1** as reference material.

Reaction Time Course Study. Incubation of MGO with N^{α}-*t*-Boc-arginine at pH 7.4 showed first rapid formation of compounds **1**, **2**, **3**, **4**, and **6** (**Figure 2**) and then degradation. In contrast, argpyrimidine (**5**) was formed slowly but continuously accumulated during time. The unidentified structures **7** and **8** reached a maximum at 6 h (1.4 mM) and were slowly degraded to give 0.4 mM at 336 h.

The pH dependency of the reaction was also investigated. Selected results are given in **Table 1**. At pH 5.0, the stability of all products was much higher (data not shown). In contrast to pH 7.4, more compound **3** than compound **2** was generated at lower reaction rates (**Table 1**). At pH 8.5, degradation of all compounds was faster and less compound **3** than compound **2** was formed. From these results, it can be concluded that the formation of compound **3** is preferred under acidic conditions, whereas the generation of compound **2** occurs under basic conditions.

Diasteriomeric isomers of compound **3** were collected separately, and the stability of these compounds was studied in separate incubations at pH 5.0, 7.4, and 8.5. Incubation of enriched compound **3b** at pH 7.4 yielded rapid formation of compound **3a** (panels **A** and **B** of **Figure 3**). After 0.5 h, a ratio of 1:1 of both isomers was reached. At pH 5.0, the reaction was slower and both isomers reached equilibrium only after 24 h (data not shown). HPLC monitoring extended incubations of isolated compound **3** demonstrated the formation of compounds **2** and **6** at pH 7.4 (**Figure 4**). This can be explained by opening the ring structure to give compound **6** and the formation of the thermodynamically more stable product **2**. At pH 5.0, the reaction was slow and yielded only low levels of compound **2** (0.4 mM after 144 h). These results were in line with the data presented in **Table 1** and underline the higher stability of compound **3** under acidic conditions, whereas ring opening and the formation of compound **2** occurs under basic conditions.

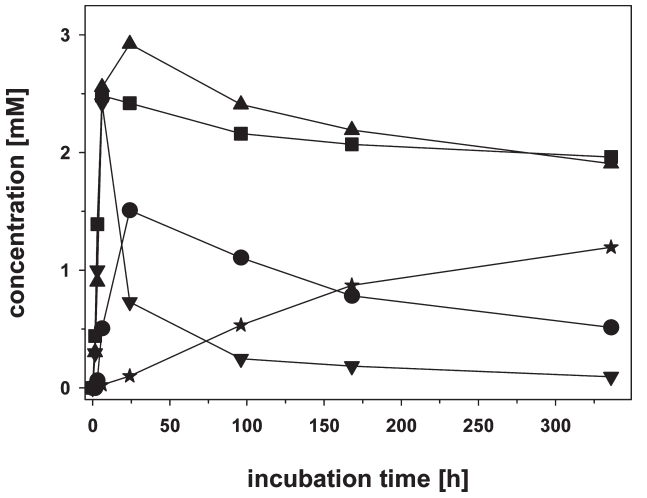

Figure 2. Concentrations of important structures during the reaction of N^{α}-*t*-Boc-arginine (20 mM) with MGO (20 mM) at 37 °C and pH 7.4: (■) N^{δ}-(4-carboxy-4,6-dimethyl-5,6-dihydroxy-1,4,5,6-tetrahydropyrimidine-2-yl)-L-ornithine (**1**), (▲) N^{δ}-(5-methyl-4-oxo-5-hydro-imidazolinone-2-yl)-L-ornithine (**2**), (▼) 2-amino-5-(2-amino-4-hydro-4-methyl-5-imidazolinone-1-yl)pentanoic acid (**3**), (★) argpyrimidine (**5**), and (●) N^{7}-carboxyethylarginine (**6**).

Table 1. pH-Dependent Formation of Compounds **2** and **3** in Incubations of N^{α}-*t*-Boc-Arginine (20 mM) with MGO (20 mM) at Maximum Concentration and at the End of Incubation (336 h) at 37 °C

	compound **2**		compound **3**	
pH	time (h)	concentration (mM)	time (h)	concentration (mM)
5.0	336	0.95	336	1.44
7.4	24	2.92	6	2.42
	336	1.90	336	0.09
8.5	24	2.12	3	0.74
	336	1.09	336	0.05

The formation of compound **4** was investigated by incubation of compound **3** with formaldehyde. Because of the N^{δ}-endocyclic ring structure of compound **4**, an acidic hydrogen at C-8 of compound **3** must be responsible for the addition of formaldehyde. As shown in **Figure 5A**, compound **3** was degraded very fast to reach 0.6 mM after 24 h. In contrast, compound **4** was formed with a maximum concentration after 6 h (1.9 mM). These findings prove the hypothesis that the reaction of compound **3** and formaldehyde leads to the aldol addition product **4**. Reaction products of compound **3** were also compounds **2** and **6**, as expected from the above separate incubation (**Figure 4**). Interestingly, incubation of compound **2** and formaldehyde did not lead to any aldol condensation product (**Figure 5B**). This suggests that compound **2** does not carry an acidic hydrogen at C-8.

The exclusive acidic hydrogen reactivity of compound **3** was confirmed when compounds **3** and **2** were incubated separately with MGO. As demonstrated in the model reaction with compound **3**, structures **1**, **2**, **5**, **6**, **7**, and **8** were found (**Figure 6**). At pH 7.4 and 37 °C, compound **3** was degraded very fast and reached a minimum level after 24 h (0.4 mM), whereas the concentration of compound **1** increased immediately and reached 2.5 mM after 24 h. The formation of compounds **6** and **2** can be explained by preferred ring opening of compound **3** and the formation of more stable products under these conditions. Compound **5** was formed slowly, and 0.5 mM was found after

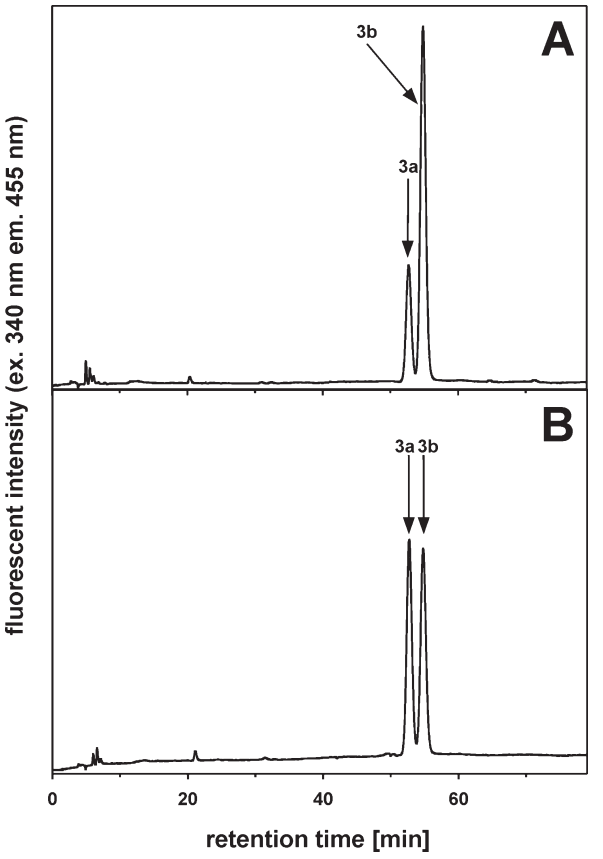

Figure 3. Incubation of enriched 2-amino-5-(2-amino-4-hydro-4-methyl-5-imidazolinone-1-yl)pentanoic acid (**3b**) after (**A**) 0 h and (**B**) 0.5 h at 37 °C and pH 7.4.

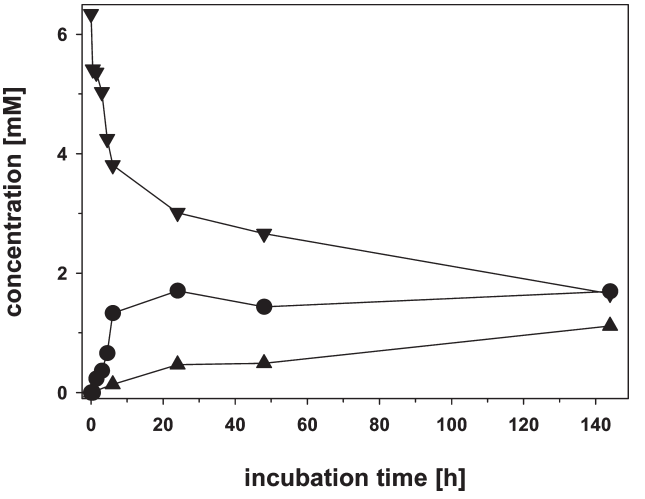

Figure 4. Degradation of compound **3** (6 mM) at 37 °C and pH 7.4: (▲) N^{δ}-(5-methyl-4-oxo-5-hydro-imidazolinone-2-yl)-L-ornithine (**2**), (▼) 2-amino-5-(2-amino-4-hydro-4-methyl-5-imidazolinone-1-yl)pentanoic acid (**3**), and (●) N^{7}-carboxyethylarginine (**6**).

144 h. Compounds **7** and **8** reached a maximum level after 6 h (1.1 and 1.2 mM, respectively) and decreased slowly. Their impact on the total reaction scheme was investigated in separate experiments described below.

Contrary to compound **3**, compound **2** did not react with MGO. The incubation of compound **2** with MGO (data not shown) was comparable to the reaction of compound **2** with formaldehyde (**Figure 5B**). There was a slight decrease of compound **2** and a

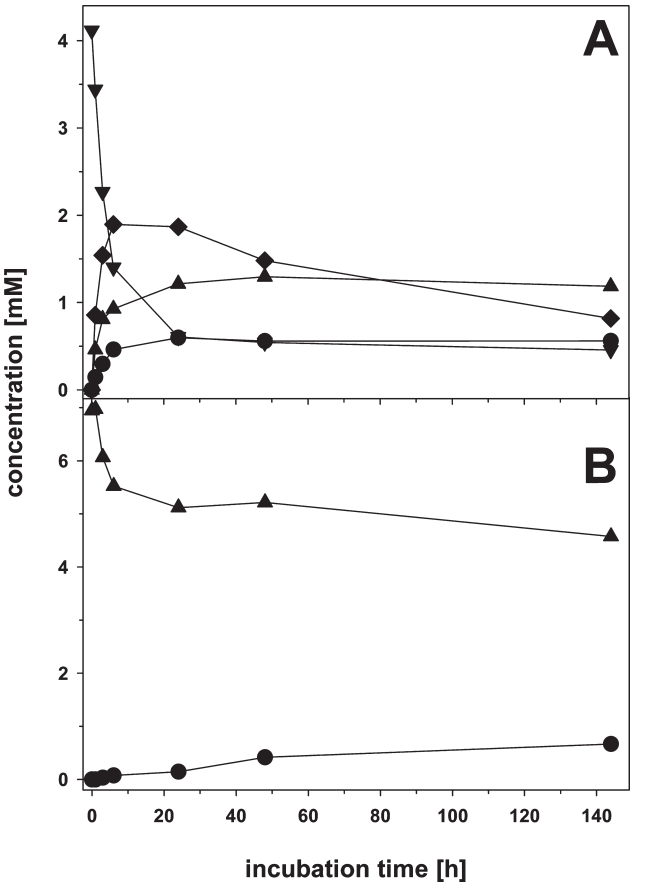

Figure 5. Incubation of MGO-derived hydroimidazolinones with formaldehyde (2.5 mM) at 37 °C and pH 7.4: (**A**) incubation of compound **3** and (**B**) incubation of compound **2**, with (▲) N^{δ}-(5-methyl-4-oxo-5-hydro-imidazolinone-2-yl)-L-ornithine (**2**), (▼) 2-amino-5-(2-amino-4-hydro-4-methyl-5-imidazolinone-1-yl)pentanoic acid (**3**), (◆) 2-amino-5-(2-amino-4-methyl-4-(methyl-ol)-5-imidazolinone-1-yl)pentanoic acid (**4**), and (●) N^{7}-carboxyethylarginine (**6**).

small increase of compound **1** (0.2 mM after 24 h), i.e., much lower compared to the reaction of compound **3** (**Figure 6**). All other structures were only negligible. Neither compound **7** nor compound **8** could be detected at all. Nevertheless, the generation of compound **1** in this incubation can be explained by the equilibrium between compounds **2** and **3**, which entails ring opening via compound **6** and allows for the addition of MGO and ultimately the formation of compound **1**. More precise information about this reaction mechanism was obtained when isolated compound **6** was incubated with MGO (**Figure 7**). Here, compound **6** was elucidated as a direct precursor for compound **1**, because major portions of compound **6** (2.7 mM after 144 h) were directly transformed into compound **1** (2.4 mM after 144 h). In contrast to the incubation of compound **3** with MGO, there were only small amounts of compounds **7** and **8** formed at later incubation times (0.7 and 0.6 mM, respectively, after 144 h).

Figure 6 shows the generation of compound **5** from the incubation of compound **3** with MGO. The detailed reaction pathway was elucidated by incubation of an isolated 1:1 mixture of compounds **7** and **8**. As demonstrated in **Figure 8**, degradation of compounds **7** and **8** lead to the formation of compound **5** up to 50% yield. The reaction was significantly slower under deaerated conditions (data not shown). Therefore, both structures must be assigned as direct precursors of compound **5**.

Theoretically, because of the pyrimidine-based chemical structure, compound **1** could be another possible precursor of compound **5**.

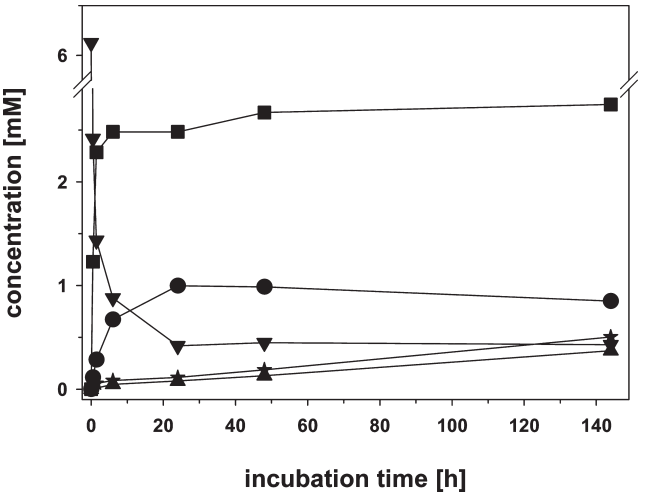

Figure 6. Incubation of compound **3** with MGO (2.5 mM) at 37 °C and pH 7.4: (■) N^{δ}-(4-carboxy-4,6-dimethyl-5,6-dihydroxy-1,4,5,6-tetrahydropyrimidine-2-yl)-L-ornithine (**1**), (▲) N^{δ}-(5-methyl-4-oxo-5-hydro-imidazolinone-2-yl)-L-ornithine (**2**), (▼) 2-amino-5-(2-amino-4-hydro-4-methyl-5-imidazolinone-1-yl)pentanoic acid (**3**), (★) argpyrimidine (**5**), and (●) N^{7}-carboxyethylarginine (**6**).

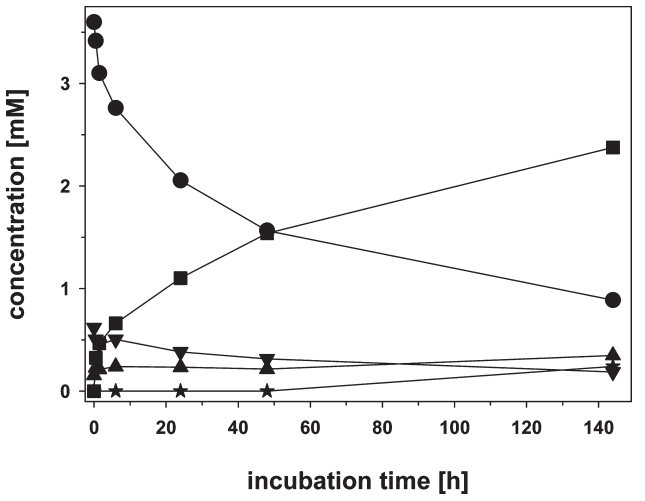

Figure 7. Incubation of compound **6** with MGO (2.5 mM) at 37 °C and pH 7.4: (■) N^{δ}-(4-carboxy-4,6-dimethyl-5,6-dihydroxy-1,4,5,6-tetrahydropyrimidine-2-yl)-L-ornithine (**1**), (▲) N^{δ}-(5-methyl-4-oxo-5-hydro-imidazolinone-2-yl)-L-ornithine (**2**), (▼) 2-amino-5-(2-amino-4-hydro-4-methyl-5-imidazolinone-1-yl)pentanoic acid (**3**), (★) argpyrimidine (**5**), and (●) N^{7}-carboxyethylarginine (**6**).

Incubation of isolated compound **1** at 37 °C and pH 7.4 rejected this hypothesis. Compound **1** was stable under the incubation conditions, and only traces of compound **5** were detectable (data not shown).

DISCUSSION

Several MGO-derived arginine modifications were determined in food and physiological samples (*17*−*19*), but little is known about their mechanistic relationship. This gave us the motivation to isolate and characterize the key players and pathways of this reaction.

From the present incubations of an equimolar mixture of MGO with N^{α}-*t*-Boc-arginine, it can be concluded that argpyrimidine (**5**) is the single only advanced glycation end product of the reaction at pH 7.4 accumulating during time. All other

structures are intermediates and were degraded after 336 h (**Figure 2**). In general, the stability of generated products was higher with decreasing pH (data not shown).

Compounds **2** (MG-H1) and **3** (MG-H3) are imidazolinone structures, which have been published before (*12*, *13*). A third imidazolinone structure [2-amino-5-(2-amino-5-hydro-5-methyl-4-imidazolon-1-yl)pentanoic acid (MG-H2)] was described as well (*13*) but could not be detected nor isolated in the present study. *In vitro* incubations of MGO with N^{α}-*t*-Boc-arginine (*20*) and lens protein (*17*), respectively, confirmed our results. In these experiments, MG-H2 isomer concentrations were only very small or not detectable. In contrast, *in vivo* investigations on glycated proteins showed a positive correlation between structure **2** and MG-H2 (*17*).

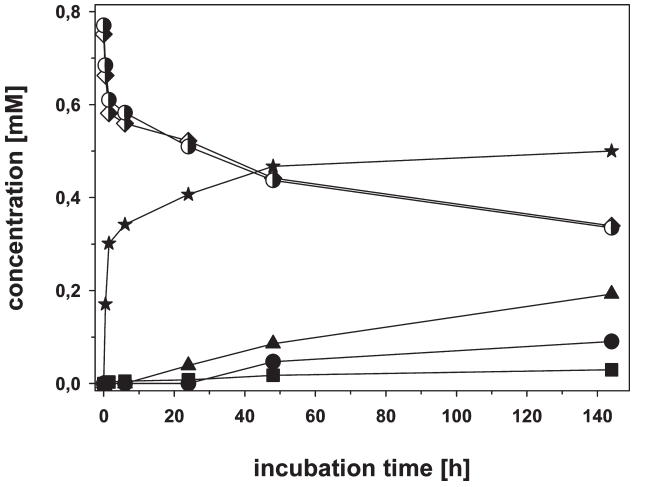

Figure 8. Incubation of compounds **7** and **8** under aerated conditions at 37 °C and pH 7.4: (■) N^{δ}-(4-carboxy-4,6-dimethyl-5,6-dihydroxy-1,4,5,6-tetrahydropyrimidine-2-yl)-L-ornithine (**1**), (▲) N^{δ}-(5-methyl-4-oxo-5-hydro-imidazolinone-2-yl)-L-ornithine (**2**), (★) argpyrimidine (**5**), (●) N^{7}-carboxyethylarginine (**6**), (half-filled diamond) compound **7**, and (half-filled circle) compound **8**.

Because compound **3** plays a key role in the generation of all other products, different experiments were focused on this compound. As shown in **Table 1**, the formation and stability of the imidazolinone structures **2** and **3** were pH-dependent. Under acidic conditions, the generation of compound **3** was preferred. In contrast, more compound **2** than compound **3** was formed with increasing pH. The same result was found in separate incubations of compound **3** at pH 5.0, 7.4, and 8.5. Under alkaline conditions, compound **2** was formed from compound **3** via compound **6** by opening the ring structure, whereas compound **3** was stable under acidic conditions (data not shown). When these results are taken together, they verified that first the reaction of MGO and arginine kinetically controlled leads to rapid and direct formation of compound **3**. With a proceeding reaction time, ring opening results in thermodynamically more stable products **2** and **6** (**Figure 9**), which was further supported by an earlier maximum of formation for compound **3** than for compounds **2** and **6** in MGO reactions (**Figure 2**). This reaction pathway was already suggested in the literature (*13*), but no experiment was performed to prove this assumption. The formation of compound **3** can only be explained via a dihydroxyimidazolidine precursor. Indeed, in the early course of arginine−MGO incubations, several short-lived intermediates evolved but could not be isolated because of their instability. Dihydroxyimidazolidine has already been described for the reaction of arginine with glyoxal (*21*). However, in contrast,

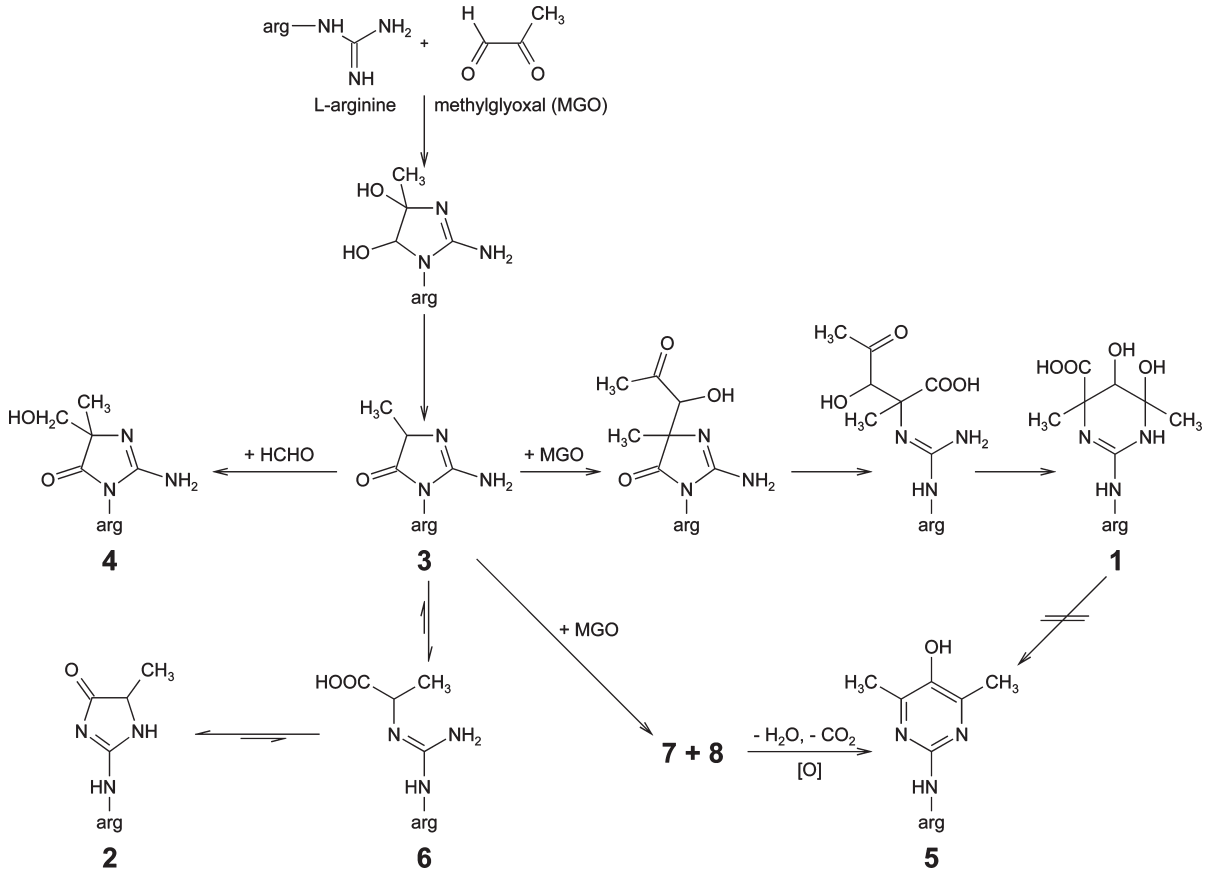

Figure 9. Formation and reaction pathways of MGO−arginine modifications.

here, dihydroxyimidazolidine represents the initial kinetically controlled intermediate ultimately leading to carboxymethylarginine as the single, stable end product of the reaction. Lo et al. (*22*) suggested that the reaction with MGO proceeds via the reversible formation of glycosylamine and dihydroxyimidazolidine. However, this alternative pathway was postulated with an exocyclic N^{δ} of the arginine residue, comparable to structure **2**, which is void based on our data.

Incubations of separated diastereomeric isomers **3** led to an immediate equilibrium of both isomers at pH 7.4 (**Figure 3**). This rapid racemization at neutral to basic pH can only be explained by an acidic proton at C-8, enabling enolic intermediates. Alternative explanations via ring opening and closure were excluded because no compound **6** could be detected at such early reaction times. Further support was the identification of aldol product **4**, as an artifact from the reaction with formaldehyde in commercially available MGO solutions. The notion that an acidic position should also be true for compound **2** was not substantiated by our experiments. Neither racemization nor aldol condensations were observed. Also, Henle et al. reported only one diastereomeric isomer for the two possible tautomeric forms of compound **2** (*12*).

The elucidation of the acidic C-8−H bond was a prerequisite to understand the formation of pyrimidine structure **1**. Incubation of compound **3** with MGO immediately led to compound **1**, the rapid kinetic identical to the formation of compound **4** from formaldehyde. In contrast, incubation of compound **6** with MGO produced a much slower but continuous synthesis of compound **1**. Taken together, this means that MGO quickly adds to C-8 from compound **3**; ring opening by hydrolysis and immediate closure then gives the obviously less strained pyrimidine derivative **1**. In the case of compound **6**, the reaction is additionally controlled by a ring closure to compound **3** to activate acidity at C-8. This mechanism is in contrast to Oya et al. (*14*), who proposed a reaction of two molecules of MGO with the guanidino group of arginine followed by cyclization via elimination of water.

A possible formation of argpyrimidine (**5**) from compound **1** is intriguing because both structures are based on pyrimidine ring systems and aromaticity would trigger the required water elimination, decarboxylation, and oxidation steps (*13*). However, on the basis of the present study, this hypothesis could not be validated. Instead, two novel structures with *m*/*z* 319 were partially isolated and elucidated as the immediate precursors of compound **5** in separate incubations. Obviously, from **Figure 6**, MGO can also add to an alternative position than C-8 to imidazolinone **3** to give compounds **7** and **8**. This reaction proceeds simultaneously but at a much lower rate than the formation of compound **1** and its precursors. The most likely alternative position of compound **3** for condensation with MGO is the exocyclic amino group. In incubations of compounds **7** and **8**, cyclization, dehydration, and decarboxylation could by verified by MS with material giving signals at *m*/*z* 301 and 257, respectively. The oxidation step was demonstrated by incubations conducted under deaerated conditions.

In conclusion, our investigations clearly identified 2-amino-5-(2-amino-4-hydro-4-methyl-5-imidazolinone-1-yl)pentanoic acid (**3**) as the single important intermediate within the reaction of MGO with arginine. Our experiments revealed unique properties of ring opening and an acidic position to allow for aldol addition with carbonyl structures first. More stable structures, such as compounds **1** and **2**, and the advanced glycation end product, arpyrimidine (**5**), were directly related to these reactions. The results were summarized in a reaction scheme for all products, part of which now has to be further substantiated by alternative isolation or synthesis of compounds **7** and **8**.

In physiological systems and foods, concentrations of MGO are often far below the amount of arginine. Therefore, MGO becomes a rate-limiting reactant, and the product spectrum will shift toward the formation of modifications involving only one molecule of the dicarbonyl compound. Another factor that might influence the product ratio is that, at the high MGO concentrations used herein, MGO monohydrate will be the preferred reactive species (*23*). However, this should not change our above general findings on reactivity and the mechanistic relationship of specific structures within the total reaction scheme.

LITERATURE CITED

(1) Hayashi, T.; Shibamoto, T. Analysis of methylglyoxal in foods and beverages. *J. Agric. Food Chem.* **1985**, *33*, 1090−1093.

(2) Mavric, E.; Wittmann, S.; Barth, G.; Henle, T. Identification and quantification of methylglyoxal as the dominant antibacterial constituent of Manuka (*Leptospermum scoparium*) honeys from New Zealand. *Mol. Nutr. Food Res.* **2008**, *52*, 483−489.

(3) McLellan, A. C.; Phillips, S. A.; Thornalley, P. J. The assay of methylglyoxal in biological systems by derivatization with 1,2-diamino-4,5-dimethoxybenzene. *Anal. Biochem.* **1992**, *206*, 17−23.

(4) Thornalley, P. J.; Langborg, A.; Minhas, H. S. Formation of glyoxal, methylglyoxal and 3-deoxyglucosone in the glycation of proteins by glucose. *Biochem. J.* **1999**, *344*, 109−116.

(5) Phillips, S. A.; Thornalley, P. J. The formation of methylglyoxal from triose phosphates. Investigation using a specific assay for methylglyoxal. *Eur. J. Biochem.* **1993**, *212*, 101−105.

(6) Richard, J. P. Kinetic parameters for the elimination reaction catalyzed by triosephosphate isomerase and an estimation of the reactions physiological significance. *Biochemistry* **1991**, *30*, 4581−4585.

(7) Thornalley, P. J. Pharmacology of methylglyoxal: Formation, modification of proteins and nucleic acids, and enzymatic detoxification—A role in pathogenesis and antiproliferative chemotherapy. *Gen. Pharmacol.* **1996**, *27*, 565−573.

(8) Lyles, G. A.; Chalmers, J. The metabolism of aminoacetone to methylglyoxal by semicarbazide-sensitive amine oxidase in human umbilical artery. *Biochem. Pharmacol.* **1992**, *43*, 1409−1414.

(9) Ahmed, M. U.; Frye, E. B.; Degenhardt, T. P.; Thorpe, S. R.; Baynes, J. W. N^{ε}-(carboxyethyl)lysine, a product of the chemical modification of proteins by methylglyoxal, increases with age in human lens proteins. *Biochem. J.* **1997**, *324*, 565−570.

(10) Nagaraj, R. H.; Shipanova, I. N.; Faust, F. M. Protein cross-linking by the Maillard reaction. Isolation, characterization, and in vivo detection of a lysine−lysine cross-link derived from methylglyoxal. *J. Biol. Chem.* **1996**, *271*, 19338−19345.

(11) Lederer, M. O.; Klaiber, R. G. Cross-linking of proteins by maillard processes: Characterization and detection of lysine−arginine cross-links derived from glyoxal and methylglyoxal. *Bioorg. Med. Chem.* **1999**, *7*, 2499−2507.

(12) Henle, T.; Walter, A. W.; Haessner, R.; Klostermeyer, H. Detection and identification of a protein-bound imidazolone resulting from the reaction of arginine residues and methylglyoxal. *Z. Lebensm.-Unters. Forsch.* **1994**, *199*, 55−58.

(13) Ahmed, N.; Argirov, O. K.; Minhas, H. S.; Cordeiro, C. A.; Thornalley, P. J. Assay of advanced glycation endproducts (AGEs): Surveying AGEs by chromatographic assay with derivatization by 6-aminoquinolyl-*N*-hydroxysuccinimidyl-carbamate and application to N^{ε}-carboxymethyl-lysine- and N^{ε}-(1-carboxyethyl)-lysine-modified albumin. *Biochem. J.* **2002**, *364*, 1−14.

(14) Oya, T.; Hattori, N.; Mizuno, Y.; Miyata, S.; Maeda, S.; Osawa, T.; Uchida, K. Methylglyoxal modification of protein. Chemical and immunochemical characterization of methylglyoxal−arginine adducts. *J. Biol. Chem.* **1999**, *274*, 18492−18502.

(15) Shipanova, I. N.; Glomb, M. A.; Nagaraj, R. H. Protein modification by methylglyoxal: Chemical nature and synthetic mechanism of a major fluorescent adduct. *Arch. Biochem. Biophys.* **1997**, *344*, 29−36.

(16) McLellan, A. C.; Thornalley, P. J. Synthesis and chromatography of 1,2-diamino-4,5-dimethoxybenzene, 6,7-dimethoxy-2-methylquinoxaline

and 6,7-dimethoxy-2,3-dimethylquinoxaline for use in a liquid chromatographic fluorimetric assay of methylglyoxal. *Anal. Chim. Acta* **1992**, *263*, 137−142.

(17) Ahmed, N.; Thornalley, P. J.; Dawczynski, J.; Franke, S.; Strobel, J.; Stein, G.; Haik, G. M. Methylglyoxal-derived hydroimidazolone advanced glycation end-products of human lens proteins. *Invest. Ophthalmol. Visual Sci.* **2003**, *44*, 5287−5292.

(18) Gangadhariah, M. H.; Wang, B.; Linetsky, M.; Henning, C.; Spanneberg, R.; Glomb, M. A.; Nagaraj, R. H. Hydroimidazolone modification of human αA-crystallin: Effect on the chaperone function and protein refolding ability. *Biochim. Biophys. Acta, Mol. Basis Dis.* **2010**, *1802*, 432−441.

(19) Glomb, M. A.; Rosch, D.; Nagaraj, R. H. N^{α}-(5-Hydroxy-4,6-dimethylpyrimidine-2-yl)-L-ornithine, a novel methylglyoxal−arginine modification in beer. *J. Agric. Food Chem.* **2001**, *49*, 366−372.

(20) Ahmed, N.; Thornalley, P. J. Chromatographic assay of glycation adducts in human serum albumin glycated in vitro by derivatization with 6-aminoquinolyl-*N*-hydroxysuccinimidyl-carbamate and intrinsic fluorescence. *Biochem. J.* **2002**, *364*, 15−24.

(21) Glomb, M. A.; Lang, G. Isolation and characterization of glyoxal−arginine modifications. *J. Agric. Food Chem.* **2001**, *49*, 1493−1501.

(22) Lo, T. W. C.; Westwood, M. E.; McLellan, A. C.; Selwood, T.; Thornalley, P. J. Binding and modification of proteins by methylglyoxal under physiological conditions. A kinetic and mechanistic study with N^{α}-acetylarginine, N^{α}-acetylcysteine, and N^{α}-acetyllysine, and bovine serum albumin. *J. Biol. Chem.* **1994**, *269*, 32299−32305.

(23) Thornalley, P. J.; Yurek-George, A.; Argirov, O. K. Kinetics and mechanism of the reaction of aminoguanidine with the α-oxoaldehydes glyoxal, methylglyoxal, and 3-deoxyglucosone under physiological conditions. *Biochem. Pharmacol.* **2000**, *60*, 55−65.

Received for review August 11, 2010. Revised manuscript received November 8, 2010. Accepted November 13, 2010.